Chapter 25

Radioactive Decontamination by Cold Plasma

- R. Kar & N. Maiti

25.1 Introduction 199
25.1.1 Conventional decontamination methods 199
25.2 Non-Thermal Plasma Etching for Radioactive Decontamination 200
25.3 Non-Thermal Plasma Chemical Etching: Case Studies 200
25.3.1 Designing atmospheric pressure non-thermal plasma devices 200
25.3.2 Brief introduction to optical emission spectroscopy (OES) 201
25.3.3 Typical optimization process of plasma chemical etching 204

25.1 Introduction

25.1.1 Conventional decontamination methods

Concerns of global warming has shifted the demand of the world towards the availability of cleaner energy sources. This trend effected in the surge of non-conventional energy sources including nuclear power industry. Electricity generation through nuclear power has seen a rapid growth in the past few decades. However, nuclear power industry has been perennially connected with the problem of safer waste management techniques. There is a perpetual difficulty in complete removal of radioactivity from various discarded/ used products before final disposal. For nuclear power industry, volume reduction of waste is the most important and they conventionally work in the principle of:

1. Dilute & disperse safely or
2. Concentrate and contain depending on the level of radioactivity.

Radioactive wastes can be in the form of solid, liquid or gas and further segregated based on the category of radioactivity. Conventional waste management methods includes either incineration or hydraulic compression of solid wastes for volume reduction. Filtration, ion-exchange, chemical treatment, solar evaporation, steam evaporation, and membrane processes are preferred for liquid wastes. Gaseous active wastes are trapped in various ways like chillers, wet scrubbers, venturi, HEPA filters. These conventional processes possess two-pronged problems:

1. Generation of high amount of secondary radioactivity and
2. Accidental exposure for workers.

These causes prompted researchers towards development of different innovative decontamination methods. Among the potential alternative techniques non-thermal/ cold plasma etching is one of the most promising methods.

25.2 Non-Thermal Plasma Etching as Non-Conventional Methods for Radioactive Decontamination

Since early nineties, researchers around the globe started testing of efficacy of non-thermal plasma etching for radioactive decontamination. Different experiments conducted on solid nuclear wastes showed that simple low pressure RF glow discharge could remove Pu; moreover, plasma was more than two hundred times faster than conventional chemical decontamination processes. Further research brought plasma etching from vacuum to atmospheric domain and the it was seen that 13.56 MHz $CF_4 - O_2 - He$ atmospheric pressure plasma could etch UO_2 from stainless steel surface. By 2010s, researchers also used 2.45 GHz, $CF_4 - O_2$ atmospheric pressure jet for radioactive decontamination. These researches established atmospheric pressure non-thermal plasma based chemical etching as a promising technology for removal of radioactive wastes for their high chemical conversion rate, favorable economics, operational easiness and lower costs. In spite of having all these advantages, this technology is not yet transferred from laboratory to nuclear power plants. In most cases, stable plasma generation requires, He as the major plasma forming gas as it is easier to create a discharge at atmospheric pressure with He compared to Argon due to presence of metastable states. However, He is around sixty times pricier than Ar, and hence, it is better to envisage a method to discharge Ar plasma even in ambient pressure. CF_4 as the etchant gas has almost been accepted universally as it is benign but releases fluorine (the most aggressive etchant) after dissociation inside plasma. It is also well-known that U and Pu are primary α-radiators handled worldwide. During etching, the basic idea remains forming hexafluoride (F_6) components of these α-emitters as hexafluoride compounds are easily evaporated between 50-60 ℃. The other fluoride components like trifluoride (F_3) or tetrafluoride (F_4) remain stable over 1000 ℃, and their formation would hinder the etching process. CF_4 as the etchant gas is benign and inside plasma its dissociation would release nascent /molecular fluorine. Nascent/molecular fluorine would then react with radioactive actinides to form hexafluoride (F_6) compounds ($U/Pu + 6F/3F_2 = U/PuF_6$). However, it is difficult to say that U/PuF_3 or U/PuF_4 would not form. Process optimization for radioactive decontamination using cold plasma thus revolves around minimizing formation of tri- and tetra-fluorides and while maximizing formation of hexafluorides. A case study on plasma chemical etching will help will help to understand it better.

25.3 Non-Thermal Plasma Chemical Etching: Case Studies

25.3.1 Designing atmospheric pressure non-thermal plasma devices

For this particular case study to understand the behaviour of plasma chemical etching, an APPJ device at 2.45 GHz will be built to understand what necessary experiments needs to be done with this device for application in nuclear industry and what is causing the limitation. Here, the power will be transferred to the device with a co-axial cable for flexibility and also the device will be made in a similar co-axial geometry. The device can be treated as a transmission line at high frequency (2.45 GHz) with its characteristic impedance $z_0 = \sqrt{\frac{L}{C}}$, where L is the inductance per unit length & C is the capacitance per unit length. Thus,

$Z_0 = 138\log_{10}(\frac{D}{d})$, where D and d are the diameters of the outer and inner conductors of the co-axial device respectively. This equation is used to design a co-axial device having impedance 50 Ω matched with the connecting cable. This device is an example of single electrode atmospheric pressure plasma jet (APPJ). One such device has been designed with

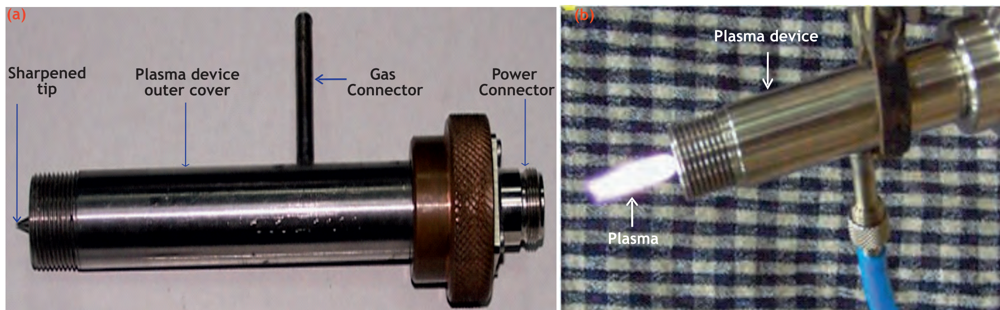

Figure 25.1: (a) Single-electrode APPJ device, and (b) Operation of single-electrode APPJ device.

an inner electrode diameter of 6.35 mm, outer cover (ground electrode) diameter of 140 mm and it exudes a plume of cross-section of 2-3 mm. Thus, single electrode APPJ device can act on a small area at one instant. For efficient increase of area of radioactive decontamination, a simple solution one can think of is increasing number of electrodes. Nevertheless, at 2.45 GHz each electrode acts as a partially independent transmission line. In such cases, calculation of L & C values manually becomes impossible and multiple electrodes also lead to interferences of propagating microwave mode through every electrode. Figure 25.2 shows pictorial representation of simulation result of a three-electrode APPJ type device. The figure below shows image of the simulated device at bottom and an impedance vs. time graph at top. Actual photograph of the operational device is exhibited on the right-hand side of the Fig. 25.2. As it is evident from the figure that this device would increase the effective plasma area compared to a single electrode device but they are more difficult to design for impedance matching. Also, high number of electrodes cause interferences of microwave modes which further creates plasma instability. One good example for increasing plasma area can be done with design of hollow cathode device operating at 13.56 MHz. Figure 25.3 shows a schematic for the principle. In the figure, the area inside the rectangle is a hollow cathode whose boundaries are equi-potential and connected to a RF source. At an instant, when the boundary is negatively charged; electrons would be repelled from this boundary. Now, if the mean free path of electron-neutral collisions at atmospheric pressure is greater than the dimension of the box, these electrons oscillate back and forth and gain energy from the source in this process till opposite cycle starts. With sufficient power, the gas inside can initiate glow-discharge plasma at ambience. This type of discharge is known as hollow cathode discharge. Size of this gap/ hollow cathode is usually between 100 μm and 400 μm. Figure 25.4 shows photograph of some RF (13.56 MHz) based hollow cathode devices.

25.3.2 Brief introduction to optical emission spectroscopy (OES)

Experiments of radioactive decontamination are usually conducted inside a glove box to contain radioactivity. Thus, initial experiments to characterize the generated plasma are conducted in a nonradioactive laboratory. Optical emission spectroscopy remains a popular technique for this purpose. It involves collection of visible radiation emitted by plasma and then use it for analysis of excited species present within plasma. If conducive conditions

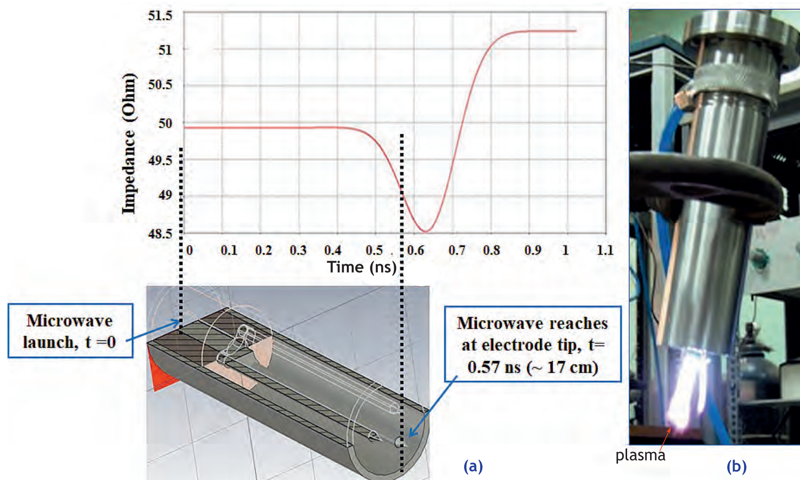

Figure 25.2: (a) Simulation showing impedance matching from back end to the electrode for a three-electrode APPJ type device and (b) the actual device with generated plasma.

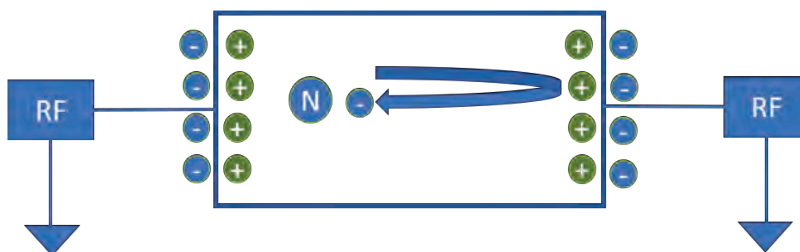

Figure 25.3: Schematic of principle for hollow cathode plasma discharge.

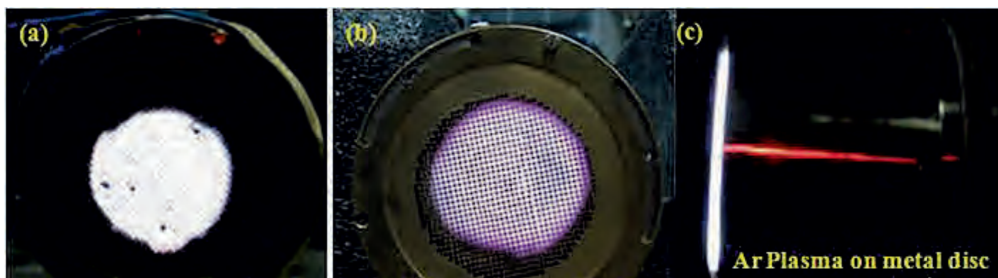

Figure 25.4: Hollow cathode-based devices with continuous increase in area of plasma: (a) 13 cm^2, (b) 16 cm^2, and (c) 32 cm^2.

are met, calculation of number and density and electron temperature is also possible from received data. The plasma however has to maintain local thermodynamic equilibrium (LTE) for this purpose. The electron temperature (T_e) in that case can be evaluated in 'two-line ratio' method. Here, if one assumes existence of two atomic ground levels (p and q) and two other excited levels (p' and q' respectively). T_e can be calculated by the following Eq.

(25.1):

$$KT_e = \frac{(E_{p'} - E_p)}{ln\left[\frac{I(p\rightarrow\ q)\ \lambda_{pq}\ A_{p'q'}\ g_{p'}}{I(p'\rightarrow\ q')\ \lambda_{p'q'}\ A_{pq}\ g_p}\right]} \tag{25.1}$$

where I is the integrated intensity, λ is the wavelength, A is the Einstein coefficient and g is the degeneracy. Number density (n_e) is usually calculated from Stark broadening of atomic lines with the assumption that Lorentzian is the sole pressure broadening existing in the system. Other assumptions are that the line is neither affected by ion dynamics nor quadratic and other higher-order Stark broadening are present. H_β (486.2 nm) is one of the atomic lines that satisfy these standards and commonly used for number density calculation from OES. An approximate analytical expression (Eq. (25.2)) used for n_e calculation is given by using FWHM of H_β line,

$$\Delta\lambda_{(1/2)}(nm) = 4.8 \times \left[\frac{N_e(m^{-3})}{10^{23}}\right]^{0.681} \tag{25.2}$$

where $\Delta\lambda_{(1/2)}$ is Lorentzian half-width half-maximum. Figure 25.5 shows the importance of OES, where this technique has been used to determine the species present in plasma (Figs. 25.5a & 25.5b), calculation of T_e (Fig. 25.5c) and n_e (Fig. 25.5d) from obtained graph.

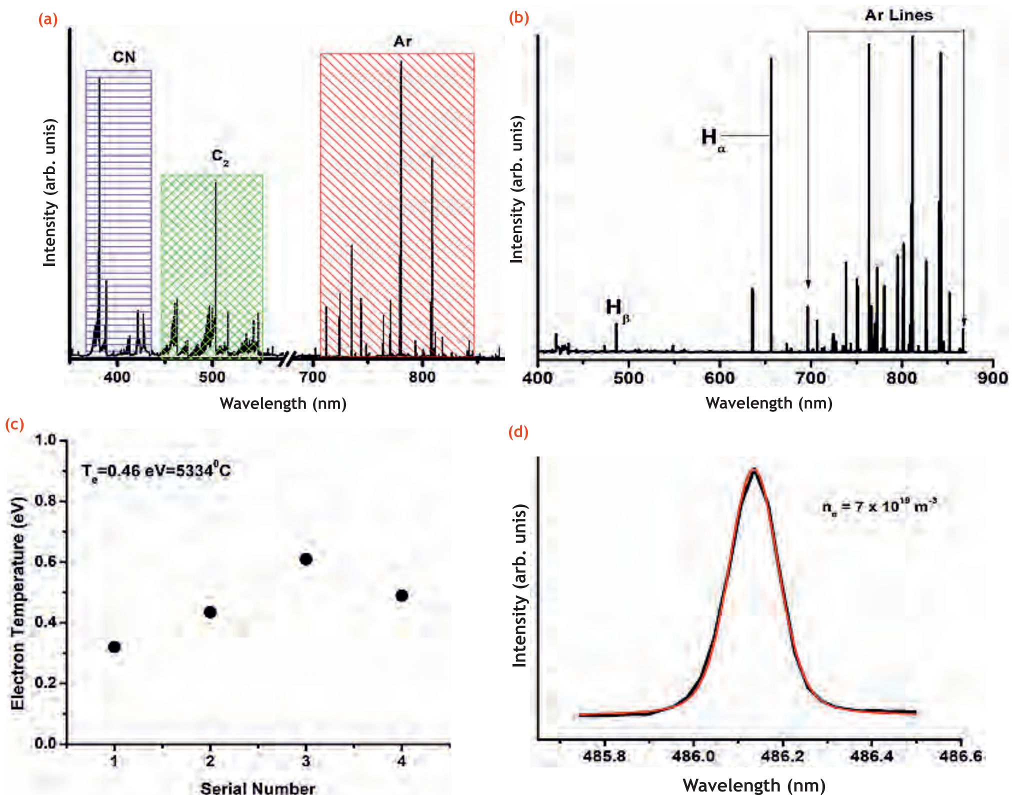

Figure 25.5: (a) Different species identified in (a) Ar + CF_4 plasma, (b) Ar + H_2 plasma (it is also used for T_e and n_e measurement), (c) Te measurement by 'two-line ratio' process, and (d) n_e measurement from H_β line.

Figure 25.6 shows OES spectrum of Ar + CF_4 + O_2 plasma and signature of CF_2

molecular bands (Fig. 25.6a), F, O atomic lines have been witnessed (Fig. 25.6b). Presence of these lines suggest that CF_4 successfully got dissociated inside plasma and released nascent F for decontamination.

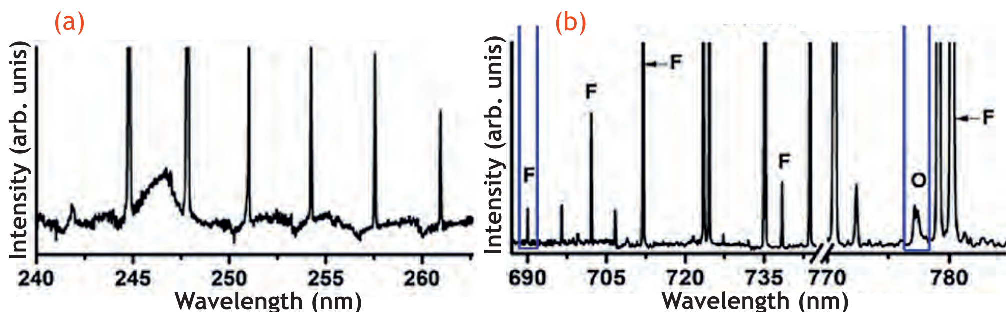

Figure 25.6: (a) CF_2 emission bands from OES spectra (240-265 nm), and (b) emission of F lines (695-785 nm), O *I* line near 777 nm also seen.

25.3.3 Typical optimization process of plasma chemical etching

Figure 25.7 shows result of cold plasma etching on Ta which is surrogate material for Pu. The images below show that the considerably smooth surface before etching (Fig. 25.7a) has been roughened up considerably after plasma etching (Figs. 25.7b & 25.7c). The images

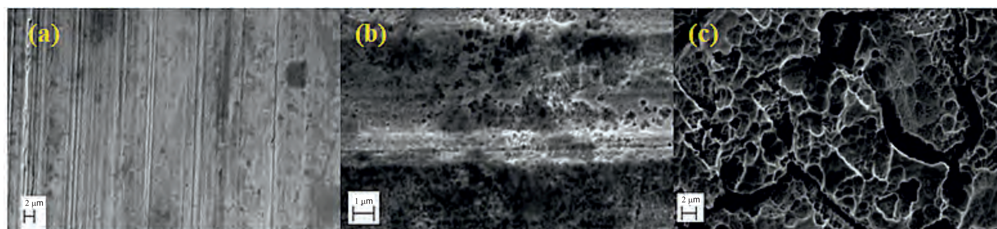

Figure 25.7: SEM images showing comparison of Ta substrates before and after etching in different conditions: (a) before etching, (b) etching without O_2, and (c) etching with O_2.

also reveal the role of O_2 on the etching efficiency. It is clearly marked that O_2 increases the efficiency of plasma etching. Figure 25.8 shows actual photograph of prepared synthetic radioactive samples. To prepare these samples, $Pu(NO_3)_4$ were put on the centre of stainless steel (SS) discs and they were heated at 800 °C. Heating helps to remove loose contamination and also diffuse radioactivity inside the sample/ substrate. Diffusion of radioactivity inside substrate volume is an important aspect to study volumetric plasma etching. Parametric optimization study is undertaken to determine exact gas ratio and operating power value to maximize decontamination factor (DF) in lowest possible time. This study is multifaceted and time-consuming. Figure 25.9 shows a dataset in graphical form. It shows changes in DF based upon changes of important plasma parameters. All data are obtained on synthetic Pu samples with a single-electrode APPJ device housed inside a glove box. Based on all these experimental results and considering maximum DF value with a stable plasma formation one arrives at the optimized experimental scheme for radioactive decontamination.

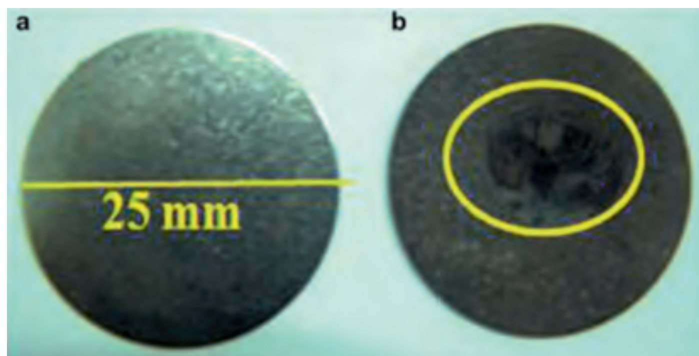

Figure 25.8: (a) SS sample (25 mm diameter) and (b) same sample with fixed Pu contamination (encircled)

Figure 25.9: Effect of various parameters on decontamination factor: (a) time, (b) CF_4 flow rate, (c) Ar flow rate, and (d) CF_4:O_2 gas ratio.

Frequently Asked Questions

Q1. Calculate number density of microwave APPJ device when Lorentzian FWHM is 0.04 nm and 0.4 nm. Compare the results and offer comments on the plasma behaviour.

Q2. Which is the best Pu surrogate material for non-radioactive lab in your opinion? Justify.

Q3. What are the advantages of plasma based radioactive decontamination compared to conventional ones?

Q4. Calculate impedance of a co-axial APPJ device for 2.45 GHz when D= 16 mm and d = 10 mm.

Q5. What are the problems associated with multi-electrode co-axial APPJ plasma device operating at 2.45 GHz?

Q6. Why synthetic radioactive samples are heated before conducting experiments?

Q7. What is the significance of taking H-beta line for number density measurement?

Q8. What are basic assumptions for calculation of two-line ratio method?